



ELSEVIER

Solar Energy Materials and Solar Cells 52 (1998) 313–344

**Solar Energy Materials
& Solar Cells**

Semiconductor thin films by chemical bath deposition for solar energy related applications

P.K. Nair*, M.T.S. Nair, V.M. García, O.L. Arenas, Y. Peña,
A. Castillo, I.T. Ayala, O. Gomezdaza, A. Sánchez, J. Campos,
H. Hu, R. Suárez, M.E. Rincón

Department of Solar Energy Materials, Centro de Investigación en Energía, Universidad Nacional Autonoma de México, Temixco, Morelos 62580, Mexico

Received 1 October 1996; received in revised form 20 May 1997

Abstract

In this paper we present the basic concepts underlying the chemical bath deposition technique and the recipes developed in our laboratory during the past ten years for the deposition of good-quality thin films of CdS, CdSe, ZnS, ZnSe, PbS, SnS, Bi₂S₃, Bi₂Se₃, Sb₂S₃, CuS, CuSe, etc. Typical growth curves, and optical and electrical properties of these films are presented. The effect of annealing the films in air on their structure and composition and on the electrical properties is notable: CdS and ZnS films become conductive through a partial conversion to oxide phase; CdSe becomes photosensitive, SnS converts to SnO₂, etc. The use of precipitates formed during deposition for screen printing and sintering, in polymer composites and as a source for vapor-phase deposition is presented. Some examples of the application of the films in solar energy related work are presented. © 1998 Elsevier Science B.V. All rights reserved.

Keywords: Thin films; Growth curves; Optical and electrical properties

1. Introduction

Chemical bath deposition technique is well suited for producing large-area thin films for solar energy related applications. In this paper we would share our

* Corresponding author.

experience in this technique, acquired at the Laboratorio de Energia Solar (presently Centro de Investigación en Energía) during the past 10 yr, with researchers in this field and others who would be interested to initiate work in this research area.

Chemical bath deposition is a technique in which thin semiconductor films are deposited on substrates immersed in dilute solutions containing metal ions and a source of hydroxide, sulfide or selenide ions. The earliest reported work dates back to 1919 and dealt with the deposition of PbS thin films [1]. The basic principles underlying the chemical bath deposition of semiconductor thin films and early research work in this area have been presented in a 1982 review article [2], which has inspired many researchers to initiate work in this area. The subsequent progress in this area is contained in a 1991 review article [3], which lists literature on more than 35 compounds prepared by this technique and related references. Recipes for the chemical bath deposition of a number of such compounds are given in a recent paper [4]. The number of possible materials to be produced through the technique is bound to multiply in subsequent years. This is due to the feasibility of producing multilayer films by this technique – the annealing of which promotes interfacial diffusion of metal ions and the production of new materials with improved thermal stabilities. For example, interfacial diffusions in chemically deposited PbS–CuS and ZnS–CuS coatings result in materials such as $\text{Pb}_x\text{Cu}_y\text{S}_z$ and $\text{Zn}_x\text{Cu}_y\text{S}_z$ with p-type conductivities and are stable up to a temperature of 300°C [5]. Annealing of Bi_2S_3 (bismuthinite)–CuS (covellite) coating at temperatures of 250–300°C leads to the formation of a new compound, Cu_3BiS_3 (wittichenite), with p-type conductivity [6].

Among the first applications of chemically deposited semiconductor thin films, we find PbS and PbSe photodetectors [7]. Even though chemically deposited CdS films were developed during 1960s, the photodetector applications of CdS were confined to screen-printed and sintered layers [8]. However, chemically deposited CdSe thin films were found appropriate for photodetector applications [9]. In the late 1970s and early 1980s the motivation in the work on chemically deposited thin films has been their prospective solar energy applications. One of the earlier developments toward this was in solar absorber coatings [10], followed by specific application of such coatings in evacuated all-glass tubular collectors [11]. Application of the chemically deposited films in solar control coatings was suggested in 1989 [12]. Subsequently the performance evaluation of such coatings was reported [13].

The use of chemically deposited semiconductor films to develop photoelectrochemical solar cells was of basic interest, most importantly, in the case of CdS and CdSe thin films [2,14,15]. Recent work on chemically deposited CdSe and Sb_2S_3 films with an incorporated WO_3 component has shown improved conversion efficiencies and stabilities in photoelectrochemical solar cell configuration [16].

The integration of chemically deposited semiconductor thin films in thin-film solar cell has only a short history. In 1990, a thin layer of chemically deposited CdS thin film was integrated into a structure Mo–CuInSe₂–CdS–ZnO producing approximately 11% of conversion efficiency [17]. This was followed by improved cell design resulting in record efficiencies of > 17% [18], in which the chemically deposited CdS film of ~0.05 μm continued to play the role of an inevitable component. The incorporation of highly resistive CdS film in the solar cell structure, (p)CuInSe₂–CdS–(n)CdS, was

identified in 1979–80 as an essential step towards improving the solar cell stability [19]. Theoretical calculations done in 1982 [20] predicted that the thickness of the CdS film should be as small as possible to increase the cell efficiency. The chemical deposition technique, which excels in providing complete surface coverage at very small film thicknesses was therefore chosen to produce this very thin film with excellent success [21].

The use of chemically deposited n-CdSe or n-Sb₂S₃ films with incorporated WO₃ phase as an active absorber material in Schottky barrier solar cells has been proven factible. For example, V_{oc} of 0.72 V; I_{sc} of 14.1 mA cm⁻²; FF of 0.7 and conversion efficiency of 5.5% have been demonstrated in ITO-(n)CdSe(5 μm)-Pt/Ni/Au(130 Å) Schottky cells [16,22,23]. Similarly, the fabrication of heterojunction solar cells using chemically deposited Sb₂S₃ thin films on (p)Si/(p)Ge/(p)InP wafers has been demonstrated [16,22,24].

The photoaccelerated chemical deposition on PbS thin films was reported in 1991 [25] in which the illuminated region in a growing thin film showed accelerated deposition. The application of this effect in producing images in PbS thin film [26] and Bi₂S₃ thin film [27] has been reported. The potential use of the photoacceleration effect in attaining high deposition rate is evident.

The above range of prospective applications, particularly, in the area of solar energy conversion and energy efficiency has prompted renewed interest in chemically deposited semiconductor thin films. The technique is ideally suited for the production of large area thin films as required for solar energy applications. In this paper we shall outline the technique for the preparation of a number of chemically deposited semiconductor thin films. The importance of post-deposition treatment in the modification of chemically deposited thin films for various applications and the prospects for producing new solar energy materials through interfacial diffusion of metal ions will be discussed. The use of the precipitate produced in the deposition bath during thin-film deposition, for the production of semiconductor coatings by other deposition techniques will also be presented.

2. Experimental

2.1. Chemical bath deposition

The basic advantages of chemical bath deposition have been highlighted by various authors [1–4,16]. The technique is applicable for the deposition of highly insoluble compounds. For example, the solubility of CuS at room temperature in water is estimated to be 10⁻³⁶ g dm⁻³, or in other words, the product of the ionic concentrations of the Cu²⁺ and the S²⁻ ions in the saturated aqueous solution of CuS is 10⁻³⁶ mol²dm⁻⁶. This is the solubility product (SP). If in an arbitrarily constituted aqueous solution of Cu²⁺ and S²⁻ ions, the product of their ionic concentration (IP) is > 10⁻³⁶ mol² dm⁻⁶, the excess ions will be precipitated as CuS. The details of these concepts are given in standard sources [28]. A list of the solubility products of sulfides and hydroxides of various metals is given in Ref. [29].

In the above-mentioned event, if the precipitation is controlled through the use of suitable complexing agents such as triethanolamine for the metal ions (so as to reduce the amount of free metal ions [30]) and the amount of sulfide, selenide, or hydroxo ions in the bath is controlled through setting up of appropriate chemical equilibria [2,3], thin-film deposition can take place. A further condition to be satisfied is the availability of nucleation centers over the substrate. Such centers are normally formed through the adsorption of metal hydroxo species over the surface. The hydroxo group would be substituted by the sulfide or selenide ions which would thereby form an initial layer of the metal chalcogenide [31]. The deposition of the thin film takes place through the condensation of the metal and sulfide/selenide ions on this initial layer, which acts as a catalytic surface.

The following compositions for the chemical deposition baths have been developed in our laboratory over many years. They have been tested for their reproducibility and have been found to be very reliable for the deposition of thin films in the thickness range 0.05–0.5 μm . The given volumes of the constituents are the quantities required to prepare 100 ml of the deposition bath. The usual substrates are microscope glass slides, 75 mm \times 25 mm \times 1 mm, cleaned in a detergent solution and rinsed well in running tap water. These are mounted nearly vertical on the wall of a 100 ml beaker containing the bath. Up to six substrates may be placed in a 100 ml beaker in this way. Deposition on a large-area commercial sheet glass may be made by slowly laying them down on a shallow tray containing the deposition bath. The sheet glass would be separated from the bottom of the tray by spacers in such a way that an approximately 5 mm thick layer of deposition bath separates the bottom surface of the sheet glass and the bottom of the tray. The thin-film deposition would take place at the bottom surface of the sheet glass. Coatings on sheet glass of 60 cm \times 60 cm are routinely made in our laboratory by this technique using approximately 2000 ml each of the deposition bath. Relatively low-cost reagents, of purity not more than 98%, are usually sufficient for the preparation of the deposition baths.

CdS thin film [32]: 30 ml of 0.1 M $\text{Cd}(\text{CH}_3\text{COO})_2 \cdot 2\text{H}_2\text{O}$, 8–12 ml of 1 M sodium citrate, 15 ml of 1.5 M NH_4OH , 5–10 ml of 1 M thiourea, and the rest deionized water to make the volume up to 100 ml. The deposition is allowed to proceed at 50–70°C for up to 12 h. Very smooth and uniform coatings of CdS are formed except at long durations of deposition.

CdSe thin films [33,34]: 30 ml of 0.1 M $\text{Cd}(\text{NO}_3)_2 \cdot 4\text{H}_2\text{O}$, 12 ml of 1 M sodium citrate, 1.2 ml of 30% (~ 15 M) NH_4OH , 0.4 g of N,N-dimethylselenourea dissolved in 30 ml of freshly prepared 0.01 M Na_2SO_3 , and the volume made up to 100 ml with water. Depositions may be made at room temperature (24 h) or at temperatures up to 60°C (8 h); at prolonged deposition there is risk of the film peeling from the glass substrates.

ZnS thin films [35]: 5 ml of 1 M zinc sulfate, 4.4 ml of $\text{NH}_3/\text{NH}_4\text{Cl}$ (pH 10), 5.4 ml of 50% triethanolamine, 2 ml of 1 M thioacetamide, and the rest deionized water to make up to 100 ml by volume. Depositions are made at 50°C for about 6 h or at room temperature for about 20 h to obtain ZnS films of 0.2 μm thickness.

ZnSe thin films [36]: 35 ml of 0.1 M zinc acetate, 16 ml of 0.8 M sodium citrate, 5 ml of 7.4 M ammonium hydroxide, and 20 ml of 0.07 M N,N-dimethylselenourea, and

the volume made up to 100 ml with deionized water. Depositions may be made at room temperature or in an oven at temperatures up to 60°C.

SnS thin films [37]: 1 g $\text{SnCl}_2 \cdot 2\text{H}_2\text{O}$ dissolved in 5 ml of acetone, 12 ml of 50% triethanolamine, 8 ml of 1 M thioacetamide, 10 ml of 4 M NH_4OH and the rest water to make up the volume to 100 ml. The depositions may be made at temperatures up to 80°C to obtain thin films of thickness 0.7 μm .

PbS thin films [38]: 5 ml of 1 M $\text{Pb}(\text{CH}_3\text{COO})_2 \cdot 3\text{H}_2\text{O}$, 20 ml of 1 M NaOH, 5 ml of 1 M thiourea, 5 ml of 1 M triethanolamine, and the rest water. The quality of films is best when depositions are done at room temperature.

Bi_2S_3 thin films [39,40]: 10 ml of ≈ 0.5 M $\text{Bi}(\text{NO}_3)_3 \cdot 5\text{H}_2\text{O}$ solution, 8 ml of 50% triethanol-amine, 4 ml of 1 M thioacetamide, and the rest water. The depositions are made at room temperature; there is risk of peeling of the film from the substrate at intermediate durations (5–7 h), but are seen to be adherent when the films are allowed to remain in the bath for more than 24 h. Improved adhesion of the films are possible when the films are deposited over a substrate layer of ZnS [35].

Bi_2Se_3 thin films [41]: 7 ml of 0.5 M $\text{Bi}(\text{NO}_3)_3$ solution, 7 ml of 50% triethanolamine, 20 ml of 0.07 M N,N-dimethylselenourea solution prepared freshly in 0.01 M Na_2SO_3 , and the rest water. Films of 0.2 μm may be deposited in about 9 h at 40°C or in about 60 h at room temperature. The films adhere well to glass substrates.

CuS thin films [42]: 5 ml of 1 M $\text{CuCl}_2 \cdot 3\text{H}_2\text{O}$, 4 ml triethanolamine, 8 ml of 30% NH_4OH , 10 ml of ≈ 1 M NaOH, 6 ml of 1 M thiourea, and the rest water. Depositions are made at room temperature for best results; the films peel from glass substrates during prolonged deposition, but it may be prevented by using a ZnS substrate film [35].

Cu_{2-x}Se thin films: 10 ml of 0.5 M $\text{CuSO}_4 \cdot 5\text{H}_2\text{O}$ solution, 1.5 ml of 30% NH_4OH , 12 ml of ≈ 0.4 M Na_2SeSO_3 solution (prepared by reflexing 4 g of selenium powder in 100 ml of 1 M Na_2SO_3 solution for about 3 h), and the rest water. At room temperature, films of approx. 0.2 μm thickness are deposited in 7 h. The value of x may depend on the exact bath composition and may even gradually change with the duration of deposition.

Sb_2S_3 thin films: 0.65 g SbCl_3 dissolved in 2.5 ml of acetone, 25 ml of 1 M sodium thiosulfate, and the rest water to make up the volume to 100 ml. The depositions were done at 10°C in a refrigerator.

The compositions of deposition baths for many other compound semiconductor thin films developed in other laboratories are summarized in Ref. [3].

2.2. Characterization

The X-ray diffraction patterns of the films were recorded on a Seimens D500 machine. The optical transmittance and the near-normal specular reflectance spectra of the samples were recorded on a Shimadzu 3101 PC UV VIS NIR spectro-photometer. For the electrical measurements, a pair of silver paint electrodes of 5 mm length at 5 mm separation were printed on the film surface to serve as contacts. The measurements were done using a computerized data acquisition system.

3. Results and discussion

3.1. Growth of thin films

In general, the growth of good-quality semiconductor thin films by the chemical bath deposition technique proceeds at a slow pace. The technique is ideally suited for producing uniform films with thickness in the 0.05–0.3 μm range in most cases. Film thickness up to a micron is possible in some cases. Thickness up to a few micron in chemically deposited CdSe and Sb_2S_3 thin films have been reported from other laboratories [16]. Higher deposition rates and higher film thicknesses are usually accompanied by powdery deposits and a lack of specular reflection. Fig. 1 shows a few examples of the films deposited in our laboratory. All the films shown in the figure are specularly reflective. The bath compositions are stated in Section 2.1.

Fig. 2 illustrates the quality of the films: the transmittance, $T(\lambda)\%$, and the specular reflectance, $R(\lambda)\%$, add up to nearly 100 at wavelengths longer than the threshold for optical absorption across the band gap. Arrows in the figure indicate the values listed for the optical band gap 1.03 eV (1204 nm) and 1.88 eV (659.5 nm) for Bi_2Se_3 and Sb_2S_3 , respectively [41,43].

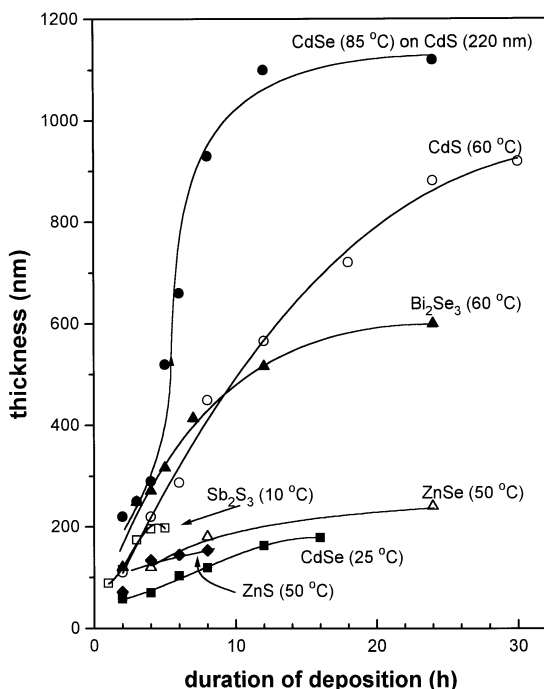


Fig. 1. Film thickness versus duration of deposition for different semiconductor thin films obtained by the chemical bath deposition technique. The bath temperature is indicated in parentheses; the bath composition is given in the text in Section 2.1.

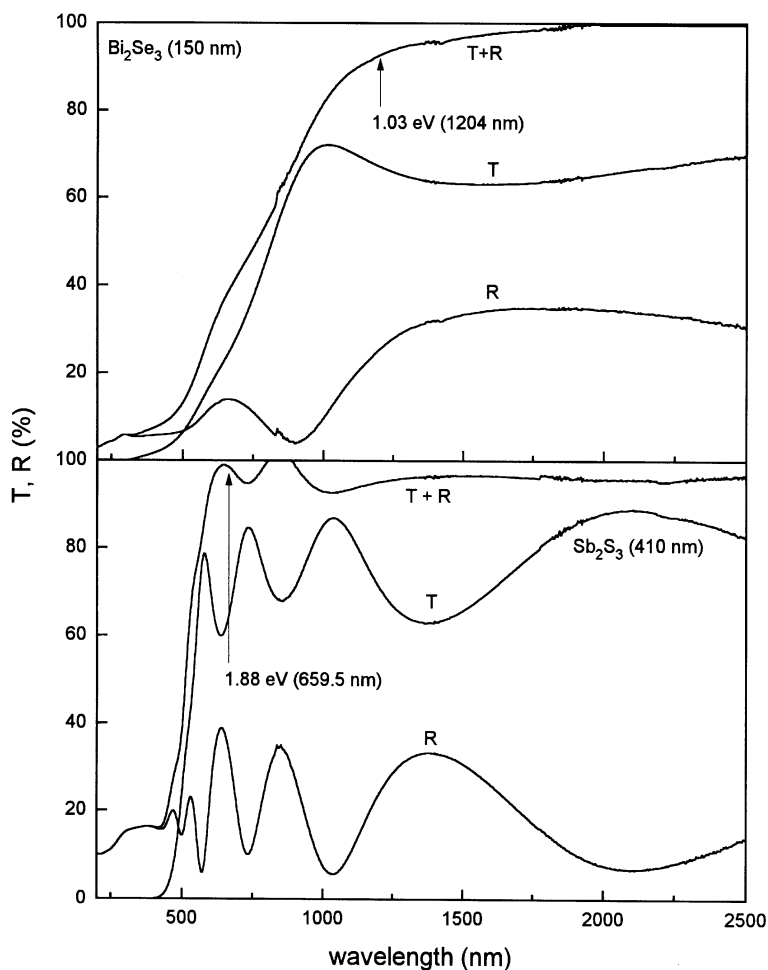


Fig. 2. The near-normal reflectance ($R\%$) and transmittance ($T\%$) curves of Sb_2S_3 and Bi_2Se_3 thin films indicating the presence of interference peaks. The sum of $R(\%) + T(\%)$ is nearly 100% at long wavelengths, indicating that the films possess nearly smooth surfaces. Arrows indicate the positions of absorption edges reported in Refs. [41,43].

3.2. Quantum confinement effect

The effect of crystallite size on the optical band gap of semiconductor thin films has been discussed by many researchers [44]. It is known that for an electron in a quantum well of width L , the quantized energy levels E_n are given by [45] $E_n = \frac{1}{2}(h/2\pi)^2 \pi^2 n^2 (m_e)^{-1} / L^2$. The ground-state energy is given by $E_1 = \frac{1}{2}(h/2\pi)^2 \pi^2 (m_e)^{-1} / L^2$, where h is the Planck's constant and m_e is the effective mass of electron. In the case of a polycrystalline semiconductor with crystalline grain width L , this leads to an enhancement of bandgap, $(E_g)_{pc}$ as compared to that of a bulk

semiconductor crystal [46]:

$$(E_g)_{pc} = (E_g)_{bulk} + \frac{1}{2}(\hbar/2\pi)^2\pi^2(m_e^{-1} + m_h^{-1})/L^2 - (1.8/\epsilon L),$$

where m_h is the effective mass for hole and the last term represents the screening term in a medium of permittivity ϵ . $(E_g)_{pc}$ approaches $(E_g)_{bulk}$ for $L > 50$ nm, but takes values considerably higher than the bulk value for $L < 5$ nm. For example, in chemically deposited CdSe films with grain sizes < 5 nm, optical band gap of up to 0.7 eV higher than the bulk value (of 1.74 eV) has been reported [47].

Fig. 3 illustrates this effect in the case of Sb_2S_3 thin films chemically deposited at 10°C . The plots of square of the optical absorption coefficient (α) versus the photon energy ($h\nu$) indicate direct band gaps for this film of about 0.7 eV higher than the bulk value (1.88 eV) for the band gap [43]. The grain size of these films are less than 5 nm; the X-ray diffraction patterns did not indicate any diffraction peak. These results for Sb_2S_3 films are in agreement with those reported by other workers [48].

3.3. Preferential orientation of the films

Preferential orientation of the crystallites perpendicular to the plane of the substrate is a common feature observed in the case of chemically deposited CdS and CdSe

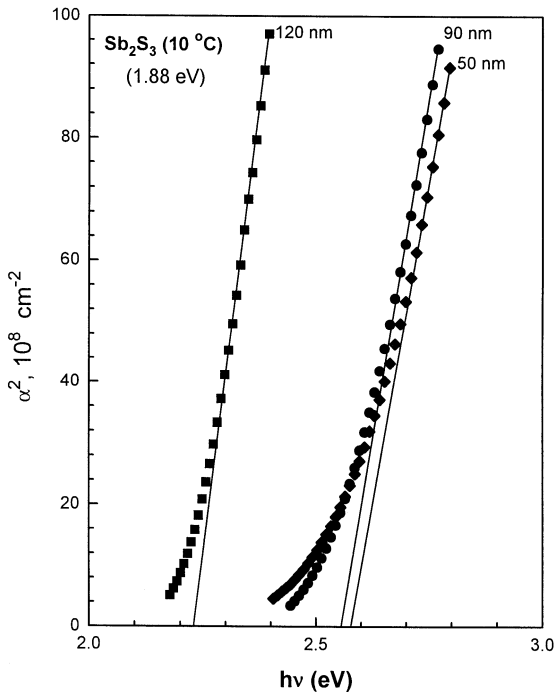


Fig. 3. The very small crystallites in chemically deposited thin films usually give rise to variation in band gaps due to quantum confinement effects; the case of Sb_2S_3 films of 50, 90, and 120 nm thickness is illustrated.

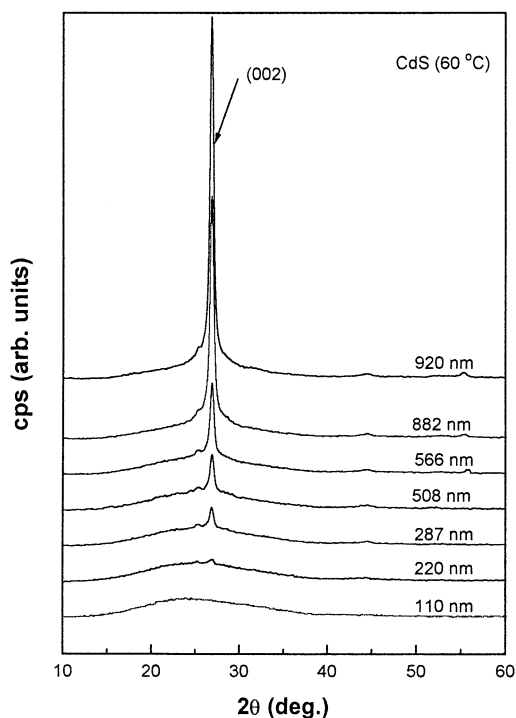


Fig. 4. Preferential orientation of the crystalline grain, with the *c*-axis perpendicular to the plane of the substrates is observed in the case of chemically deposited thin films in the thickness range 110–920 nm.

thin films. Fig. 4 shows the typical case of CdS thin films deposited at 60°C, using citrate as a complexing agent as described in Section 2.1. The orientation is so pronounced that only the diffraction peak corresponding to the (0 0 2) planes is noticeable. The figure also shows that at very small film thicknesses the films appear to be amorphous or possess very small crystallites.

3.4. Photocurrent response

Fig. 5 shows the photocurrent response of a number of chemically deposited thin films. Except for CdS, the films do not exhibit large changes in the current upon illumination. Most films are highly resistive in the dark; the electrical conductivities in the dark range from 10^{-8} to $10^{-6} \Omega^{-1} \text{ cm}^{-1}$. Exceptions are CuS and Cu_{2-x}Se thin films: the film conductivities are in the 10^3 to $10^4 \Omega^{-1} \text{ cm}^{-1}$ range. Such high electrical conductivities produce free carrier absorption in the infrared region, very small optical transmittance and high reflectance in the infrared region. These features in the optical transmittance and reflectance spectra are shown in Fig. 6. The high electrical conductivity arises from copper deficiency in the films, which make them p-type [49]. This is a feature of copper chalcogenide films prepared by vacuum-based

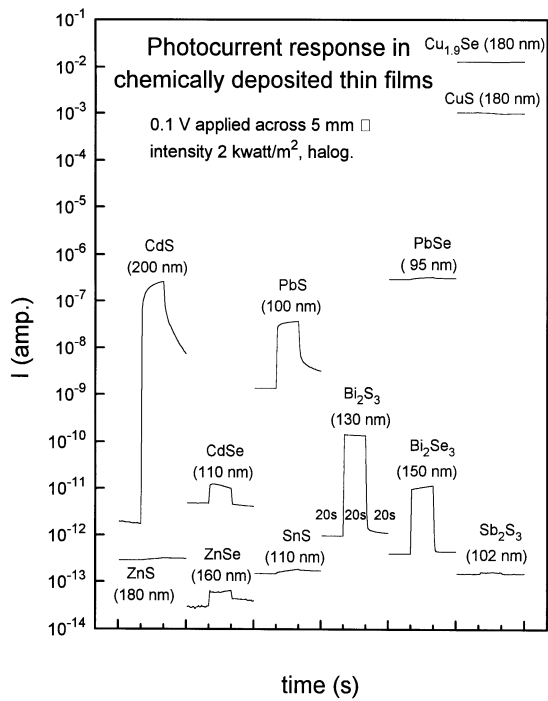
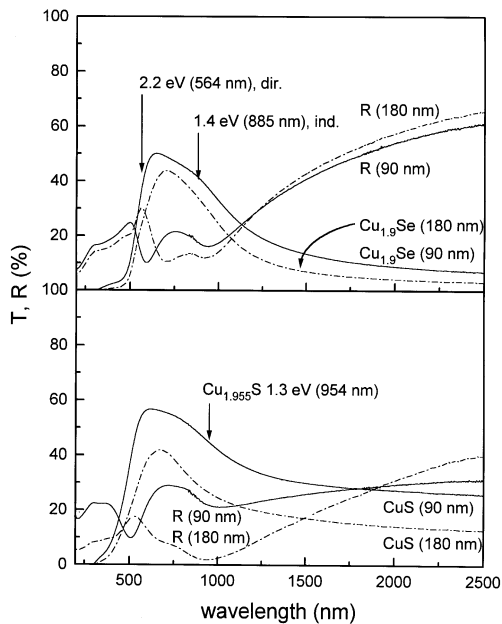


Fig. 5. Photocurrent response of various semiconductor thin films prepared in our laboratory by chemical bath deposition technique.



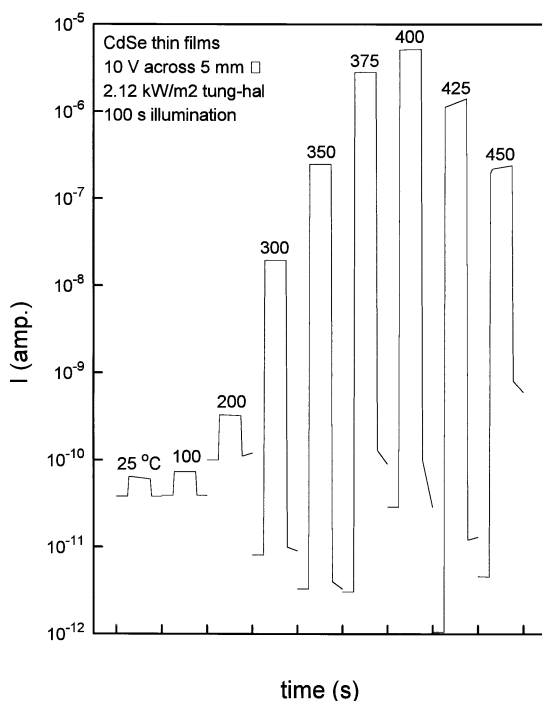


Fig. 7. Variation in the photosensitivity of the films produced by annealing of a CdSe film (~ 150 nm) in air for 1 h each at different temperatures.

techniques as well [50]. The optical characteristics such as the one presented in Fig. 6 have been found to be ideal for application of these films in solar control glazing [51].

3.5. Effect of air annealing on the photo response curves

Air annealing leads to significant changes in the chemical, structural, electrical, and optical properties of chemically deposited semiconductor thin films. Notable examples are the following:

CdSe thin films: The as-prepared thin films possess very poor photosensitivity: $S = (I_{ph} - I_d)/I_d$, where I_{ph} and I_d are the photocurrent and dark current, respectively. The CdSe thin films ($\sim 0.18 \mu\text{m}$ thickness) in Fig. 7 were deposited at room temperature using *N-N*,dimethylselenourea as the source of selenide ions [33,34]. The photosensitivity increases from about 0.5 in as-deposited films to approximately 10^6 after the film has been annealed in air at 375–425°C for 1 h. This increase in

Fig. 6. Transmittance ($T\%$) and near-normal reflectance ($R\%$) curves of chemically deposited CuS thin films and Cu_xSe thin films, indicating the high near-infrared reflectance and low infrared transmittance caused by the high electrical conductivities ($\sim 10^3 \Omega^{-1} \text{cm}^{-1}$) of the films shown in Fig. 5. Arrows indicate the positions of absorption edges reported in Ref. [43] for the materials of compositions shown.

photosensitivity arises from the combined effect of grain size growth and chemisorption of oxygen in the intergrain region as discussed in earlier papers [33,34]. The mechanism of enhancement of charge carrier mobility in polycrystalline thin-film semiconductors as a function of grain size and illumination have been the subject of many earlier studies [52,53]. In short, the chemisorbed oxygen at the intergrain region builds up repulsive potential for the transport of electrons, leading to very low electron drift mobilities and hence produces only very small electric currents. Illumination produces electron–hole pairs, of which the holes neutralize the repulsive potential at the grain boundaries and leads to an exponential increase in the electron mobility. This results in a high photocurrent under illumination which combined with the very low current in dark produces a high photosensitivity in the films.

CdS thin films: In sharp contrast with the effect of air annealing on the photosensitivity of CdSe thin films, the photosensitivity of the CdS thin films degrades under the same annealing process. Fig. 8 shows that the photosensitivity of as-prepared films is nearly 10^8 , but annealing at temperatures 300–400°C lowers it to 10^3 – 10^4 . Annealing at higher temperatures improves the electrical conductivity drastically, as reported previously [31]. The increase in conductivity arises from the formation of a top layer of CdO, which is highly n-type due to incomplete oxidation

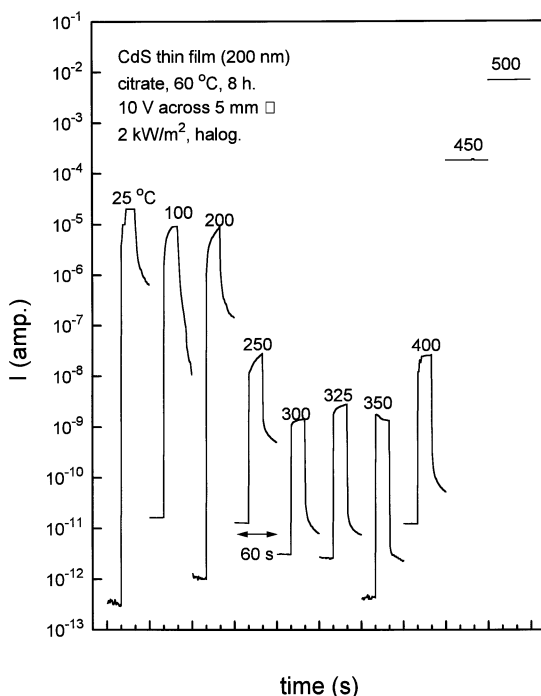


Fig. 8. Effect of annealing in air for 1 h each at different temperatures of a CdS thin film (200 nm) on the photocurrent response curves; the high electrical conductivities ($\sim 50 \Omega^{-1} \text{ cm}^{-1}$) of the film obtained after annealing at 500°C results from a partial conversion of the CdS films to a nonstoichiometric CdO_{1-x} film.

which renders the CdO layer excess in Cd. X-ray photoelectron spectroscopy studies indicated that the CdO surface layer resulted from the CdS film [31], and the X-ray diffraction studies showed that the conversion could not be completed during the air annealing process – the presence of the underlying CdS film could be detected along with the CdO component. Assuming that the CdO film thickness is of about 100 nm (over the CdS film) in the case of the film annealed at 500°C in Fig. 8, the electrical conductivity is seen to be approximately $100 \Omega^{-1} \text{ cm}^{-1}$. Same range of conductivity is observed in CdO films produced by the oxidation of chemically deposited $\text{Cd}(\text{OH})_2$ films [54]. Annealing the CdS films, prepared by the citrate method, in an inert atmosphere is yet to be studied. It may be possible to identify the optimum annealing conditions which would result in improvement in the grain size and hence enhance the photoconductivity in these films without decomposition to oxide.

ZnS thin films: Fig. 9 shows that the ZnS thin films of about 200 nm deposited at 25°C are very resistive; sheet resistance is of nearly $10^{12} \Omega/\square$ and electrical conductivity (dark/photo) is nearly $10^{-8} \Omega^{-1} \text{ cm}^{-1}$. Air annealing for 1 h at 388°C increases the photosensitivity to $\simeq 10^4$ and annealing at 450°C for 1 h increases the photoconductivity to $> 0.05 \Omega^{-1} \text{ cm}^{-1}$. The formation of a ZnO layer has been indicated by X-ray diffraction studies. The formation, however, is not complete. XRF studies have shown

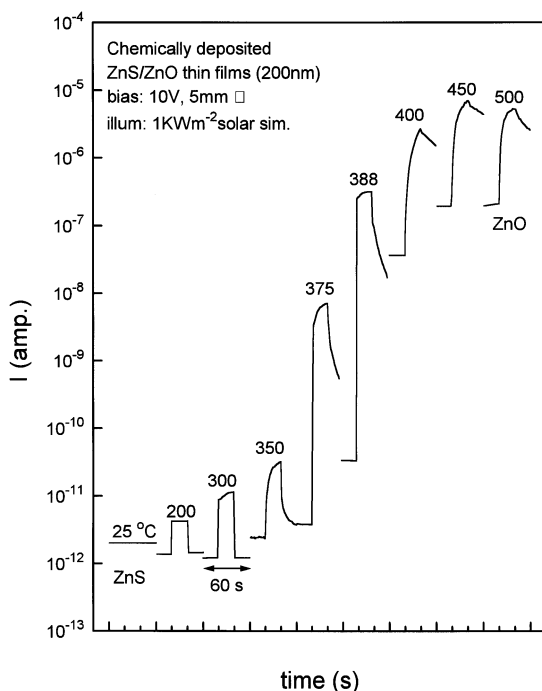


Fig. 9. The conversion of as-deposited, nonphotosensitive, ZnS thin film (200 nm thickness) to photo-sensitive thin film by air annealing at 375–388°C, beyond which the films are partially converted to nonstoichiometric ZnO thin film, leading to electrical conductivities $> 0.01 \Omega^{-1} \text{ cm}^{-1}$.

the presence of about 30% of the initial sulfur content in the films after they were annealed at 450°C–500°C for up to 2 h. Thus, the ZnO is formed as a surface layer. The high conductivity arises from the incomplete oxidation, ZnO_{1-x} , similar to the case of CdO films. Fig. 10 shows that the ZnS–ZnO thin film maintains a high optical transmittance $\sim 80\%$ in the near-infrared region and shows a shift in the optical band gap toward lower values. The α^2 versus $h\nu$ plots for the film indicate band gap values of about 3.7 eV for the as-prepared and 3.4 eV for the ZnS–ZnO film produced by air annealing at 500°C for 1 h.

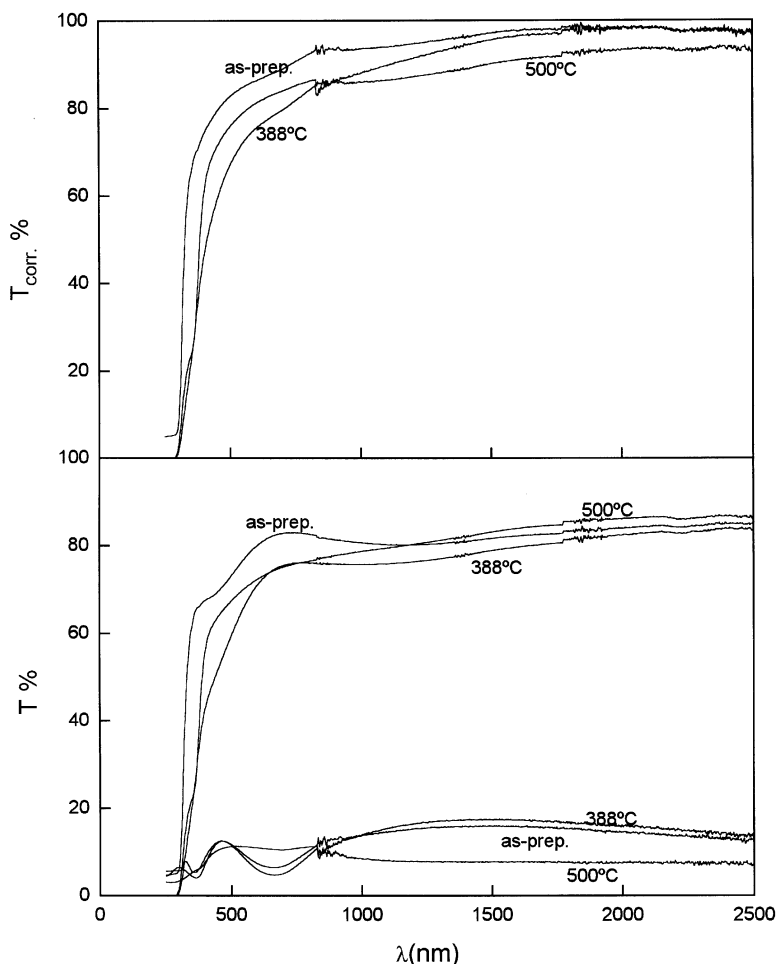


Fig. 10. The optical transmittance and reflectance spectra of a chemically deposited ZnS thin film, showing that the as-prepared and annealed (ZnS/ZnO) films possess high optical transmittance ($T_{\text{corr.}}(\%)$; $T_{\text{corr.}}(\%) = 100 T\% / (100 R\%)$).

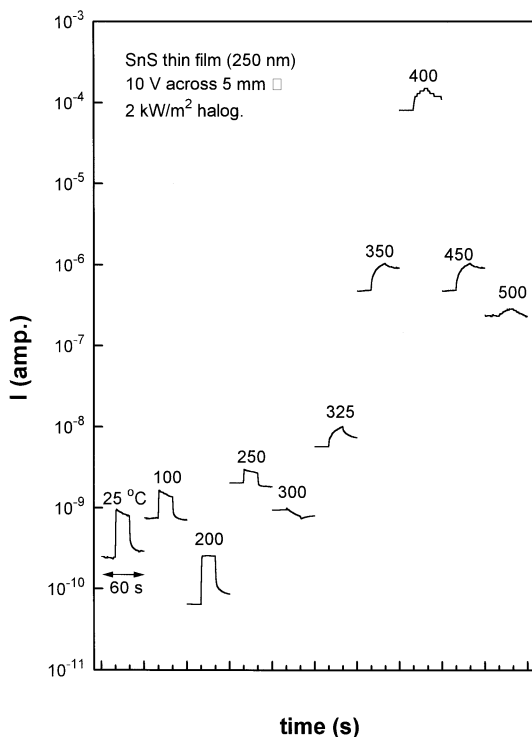


Fig. 11. Conversion of chemically deposited SnS thin films (250 nm) to SnO₂ films (400–500°C) by air annealing.

SnS thin films: The as-prepared films in this case are very resistive. Annealing at about 300°C leads to the partial conversion of SnS to SnO_{2-x}; the nonstoichiometry leads to high electrical conductivities. The proportion of SnO_{2-x} in the film increases with temperature. Fig. 11 shows that at 400°C the conductivity of the film is the highest, about $0.5 \Omega^{-1} \text{ cm}^{-1}$. At this annealing temperature the SnS thin film, which originally appears orange-red in transmitted daylight becomes nearly transparent [55]. Annealing at temperatures above 400°C retains the film transparent, but leads to a better stoichiometry, SnO₂, which increases the resistance of the films.

3.6. Conversion of chemically deposited films to n-type by ion exchange reactions and diffusion of indium

In earlier papers we have discussed that immersion of CdS thin films in a dilute solution (0.05 M) of HgCl₂ for a few minutes and annealing in air at 200°C for a few minutes produces n-type conductivity of $\sim 1 \Omega^{-1} \text{ cm}^{-1}$ in the films [31]. This conductivity is stable during storage in desiccator over a period of several months. Similar improvements in electrical conductivity are observed in CdSe thin films as

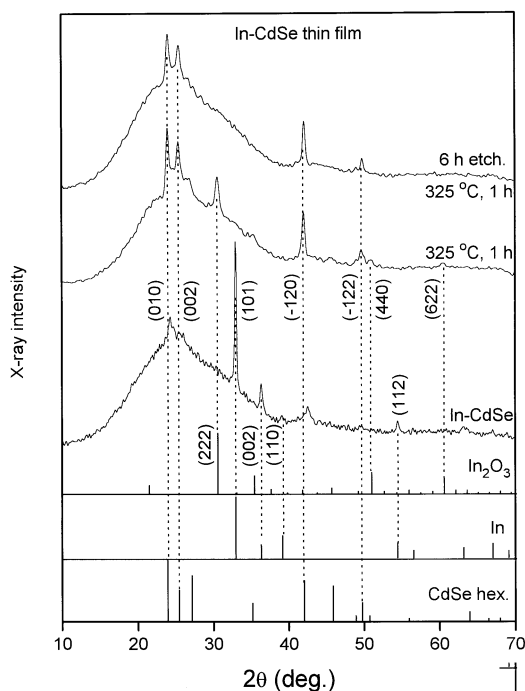


Fig. 12. Conversion of chemically deposited CdSe thin films to n-type through deposition of a 20 nm indium film on the CdSe film (150 nm) and subjecting it to air annealing at 325°C for 1 h. A chemical etch for 6 h in a 1 M HCl solution removes the top In₂O₃ layer, which exposes the underlying CdS:In layer.

well [56]. The increase in conductivity has been attributed to the incorporation of chlorine in the film. The drawback of this type of conversion to n-type is loss of the conductivity at higher annealing temperatures (300°C or above).

Recently, we reported another technique to convert the chemically deposited CdS [57,58] and CdSe thin films to n-type [59]. Fig. 12 illustrates the basic mechanism involved. A 20 nm thick indium film is evaporated over a chemically deposited CdSe thin film of about 150 nm thickness [59]. The quantity of indium required for this is about 15 mg to cover an area of 150 cm² of the film surface. Annealing at 300–350°C produces an In₂O₃ surface layer, which may be removed by etching in 1 M HCl solution. The underlying film is indium-doped CdSe, i., CdSe:In. Fig. 13 shows that the conductivity of such a film is high: nearly $1\Omega^{-1}\text{cm}^{-1}$ as compared to that of the CdSe film ($10^{-7}\Omega^{-1}\text{cm}^{-1}$) annealed in air under the same conditions. The conductivity was found to be stable during desiccated storage.

Fig. 14 shows that thermal diffusion of indium does not inevitably produce n-type conductivity by substitution of a divalent metal in chemically deposited thin films. In the case of a 20 nm indium film deposited over a PbS thin film, metallic lead is

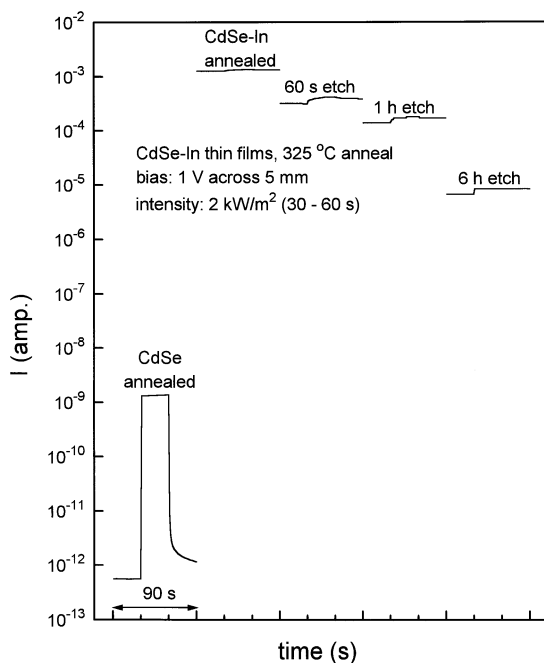
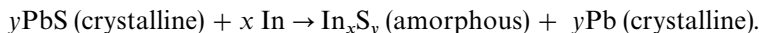


Fig. 13. Photocurrent response of annealed CdSe–In films, showing that a conductive In_2O_3 layer is formed on the film, which can be etched away in 1 M HCl solution. The underlying film after a 6 h etch is devoid of the In_2O_3 film (Fig. 12), but possesses a dark conductivity of $3 \Omega^{-1} \text{ cm}^{-1}$, nearly seven orders of magnitude higher than that of a CdSe film annealed under the same conditions.

precipitated in the medium, resulting from a reaction of the type



This reaction takes place when the films are annealed at 300°C , and produces a composite material. The conductivity of this film is high: $500 \Omega^{-1} \text{ cm}^{-1}$ and sheet resistance is about $100 \Omega^{-2}$.

3.7. Conversion of chemically deposited thin films to p-type by ion exchange reactions and interfacial diffusion

The conversion of chemically deposited CdS thin films to p-type by topotaxial reaction in a CuCl solution of pH 3.7 at 90°C for about 10 s has been developed as a method to produce CdS– Cu_2S solar cells in the 1980s [60]. The incorporation of copper ions in chemically deposited CdSe thin films by immersion in a dilute solution of CuCl_2 (0.005 M) has been reported before [56] from our group. The presence of $\text{Cd}_x\text{Cu}_y\text{Se}_z$ composition in the surface layer, as evidenced in the XPS studies, gives rise to very low sheet resistance (and of p-type conductivity) of $10^5 \Omega/\square$ as compared to $10^{12} \Omega/\square$ of the CdSe films. The same is the case with ZnSe thin films as well:

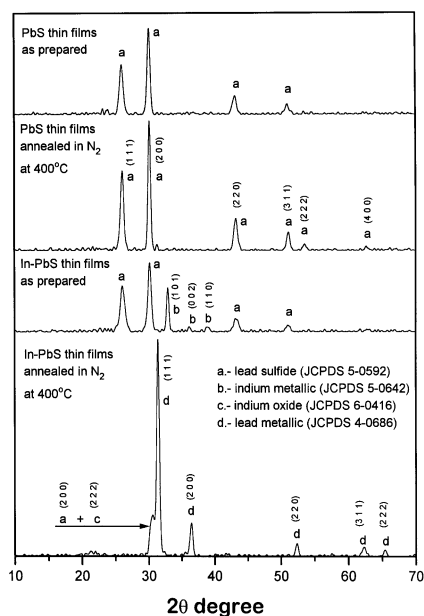
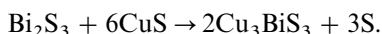


Fig. 14. XRD patterns illustrating that annealing in nitrogen of a PbS (200 nm) – In (20 nm) film results in the formation of metallic lead crystallites and the dispersion of indium in the matrix; the presence of which is detected in the X-ray fluorescence spectra.

immersion for about 1 min of a ZnSe thin film in a 0.025 M CuCl_2 solution reduces the sheet resistance from about $10^{12} \Omega/\square$ to $10^3 \Omega/\square$ through the formation of a $\text{Zn}_x\text{Cu}_y\text{Se}_z$ composition on the surface layer [61].

Production of thermally stable thin films of p-type conductivity of about $300 \Omega^{-1} \text{cm}^{-1}$ (sheet resistance of about $100 \Omega/\square$) is possible through interfacial diffusion of metal atoms in ZnS–CuS or PbS–CuS multilayers [5]. The films are stable in the temperature range 150–350°C under air annealing. More interesting results were obtained when Bi_2S_3 –CuS films were annealed. The formation of a new compound Cu_3BiS_3 (wittichenite) was suggested in a previous paper [62] and detailed results are presented in a recent paper [6]. Fig. 15 illustrates the mechanism of formation of the new film. Annealing the Bi_2S_3 –CuS films at temperatures of 200–300°C results in the interfacial diffusion of metal ions and formation of the new compound through the reaction



The excess sulfur may be removed by immersion in a suitable solvent. The conductivity of the resulting film is $> 100 \Omega^{-1} \text{cm}^{-1}$. This indicates that many chemically deposited thin films involving Cu_{2-x}Se , CuSe, CuS and Cu_xS may be subjected to suitable annealing process to produce multinary compounds.

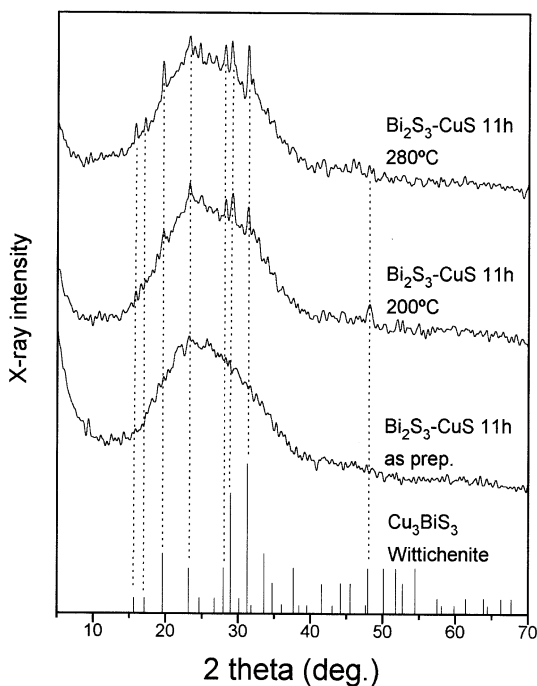


Fig. 15. The formation of a new material, Cu_3BiS_3 (mineral sample; wittichenite) during annealing at $200\text{--}280^\circ\text{C}$ of a chemically deposited $\text{Bi}_2\text{S}_3\text{-CuS}$ thin film (X-ray source, Cu K_α).

3.8. Use of the precipitate as a precursor for other coating techniques

The real challenge in the optimization of a chemical bath deposition technique is to reduce the particulate precipitate in the bath obtain in high thin-film yield. Nevertheless, even in the best optimized bath, precipitate presents itself as a major product of the condensation process. The precipitate may be filtered and reacted with acids to produce the starting materials for deposition. But, in many cases the precipitate may be rinsed well, dried and stored to serve as precursor for other deposition techniques. Following are the three specific examples:

(i) *Screen printing technique*: The basic principles involved in screen printing process for producing semiconductor coatings have been discussed in Ref. [63]. This technique has been successfully used in the production of CdS-CdTe solar cells [64]. The screen printing process involves the preparation of a paste containing the semiconductor pigment, a flux material which will fuse at a temperature much below the melting point of the pigment, and a binder usually ethylene glycol or propylene glycol. The paste is printed on suitable substrates using a silk screen or polyester screen, dried for a few hours at $50\text{--}80^\circ\text{C}$, and then sintered at a temperature higher than the melting point of the flux. Fig. 16 illustrates the physicochemical changes that occur during the sintering process [65]. Here, CdSe precipitate recovered from a chemical deposition bath [33,34] was mixed with 30% by weight of ZnCl_2

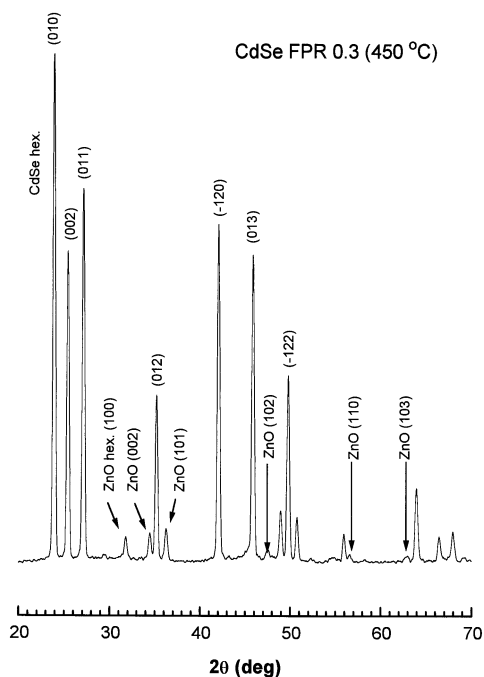


Fig. 16. X-ray (Cu K_α) diffraction pattern of a screen-printed and sintered (450°C) CdSe/ZnO layer prepared using CdSe precipitate and 30% by weight of ZnCl_2 as flux (flux-to-pigment ratio, FPR = 0.3) dispersed in propylene glycol.

(anhydrous) and sufficient quantity of propylene glycol to produce a screen printing paste. The paste was screen printed on to glass substrates using a 120 T polyester screen (approx. mesh: sieve opening $44\ \mu\text{m}$ and filament diameter $30\ \mu\text{m}$). The coating was dried in an air oven at 110°C for 1 h and sintered at $350\text{--}450^\circ\text{C}$ in air for 1 h each. The XRD pattern in Fig. 16 for the coating sintered at 450°C shows well-defined peaks of CdSe and ZnO. A possible mechanism is that at temperatures above the melting point of ZnCl_2 , it melted and covered the CdSe pigment. At the sintering temperature ZnCl_2 combined with atmospheric oxygen forming ZnO. XRF studies have indicated that the chlorine content of the film has been significantly reduced in the sintered film – up to 10% of its original value in the dried screen printed coating.

Fig. 17 illustrates the high photosensitivity achieved in the screen printed film prepared as above. The best photosensitivity, $\sim 10^8$, is obtained for a sintering temperature of 450°C . Photosensitivity of even higher than this (for example, 10^9 under air mass one solar radiation) has been obtained in chemically deposited CdS thin films [66,67]. However, the fast decay of photocurrent of the screen printed CdSe/ZnO coatings is not matched by them.

(ii) *Use in the production of composite coatings:* Fig. 18 shows the sheet resistance of composite coatings made of CuS pigments precipitated from a chemical bath used for thin-film deposition [42] dispersed in poly(acrylic acid) (molecular weight assay

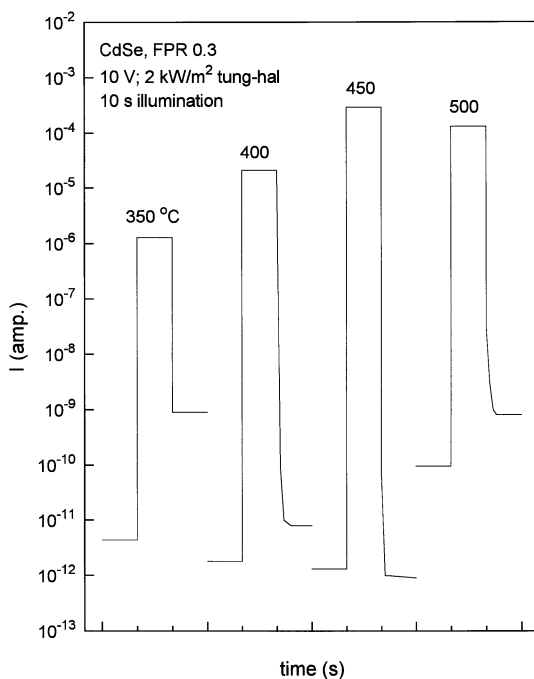


Fig. 17. Photocurrent response (10 s dark, 10 s illumination, and 10 s dark) of the screen-printed CdSe/ZnO coating as a function of sintering temperature.

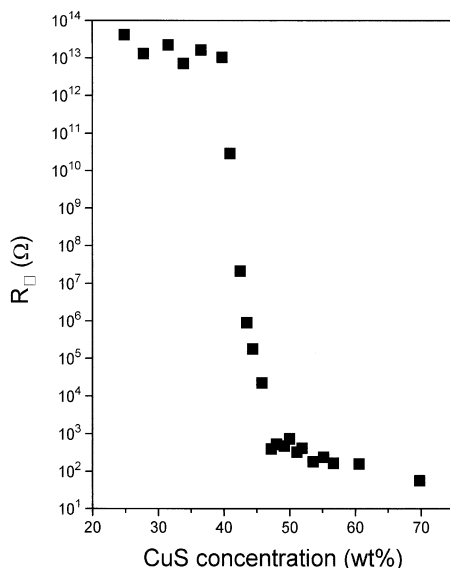


Fig. 18. Sheet resistance of CuS–polyacrylic acid composite coatings, where the CuS precipitate was obtained from a chemical deposition bath. The CuS weight percentage indicates the percentage weight of CuS component in the total weight of the composite, poly (acrylic acid) plus the precipitate.

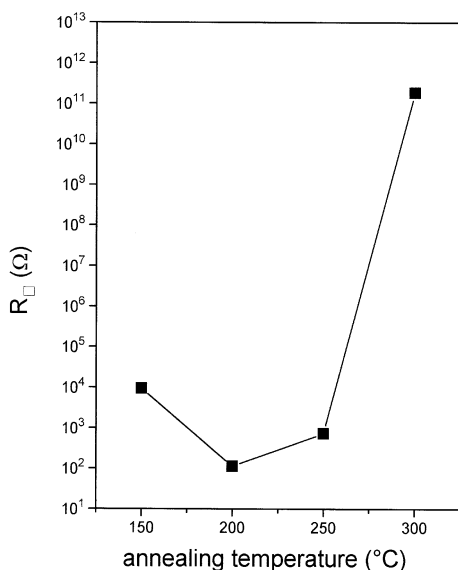


Fig. 19. Variation of sheet resistance in CuS–poly acrylic acid composite coatings with temperature of annealing.

90 000), with propylene glycol used as a solvent. The conductivity percolation is seen at 40% w/w of CuS powder in the total weight of the composite. Sheet resistance of nearly $100 \Omega/\square$ is obtained at a wt% of about 55% CuS. Higher wt% of the precipitate makes the surface of the coating rough. The results shown are for coatings annealed at 200°C . Fig. 19 shows that the conductivity does not degrade considerably when annealed at a temperature up to 250°C . Above this, there is chemical conversion of the CuS component to digenite, Cu_9S_5 , (JCPDS 26-0476) as illustrated in Fig. 20 and a transition of the coating to an insulator. The conversion may take place through the release of sulfur into the polymer matrix, for example, $15\text{CuS} \rightarrow 6\text{CuS} + \text{Cu}_9\text{S}_5 + 4\text{S}$. The resulting changes in chemical bonding have been studied by FTIR and discussed in Ref. [68].

(iii) *Use of the precipitate as the source for vapor phase deposition:* The semiconductor precipitate produced in the chemical deposition bath is, in general, stoichiometric. The purity of the precipitate is superior to that of the starting chemicals in the bath because the impurities whose concentrations are below those required for precipitation into solid phase (i., ionic product < solubility product) are left behind in the solution. Thus, the precipitate can serve as a relatively pure source of semiconductor material for vapor phase deposition. In a recent study we used the bismuth sulfide precipitate recovered from a bath [39] normally used for depositing thin films. The dried powder was placed in the center zone of a tubular vacuum furnace (10 mTorr) and heated to 500°C . Glass substrates were placed along the axis of the tubular furnace from the center of the furnace downstream toward the pumping outlet, with

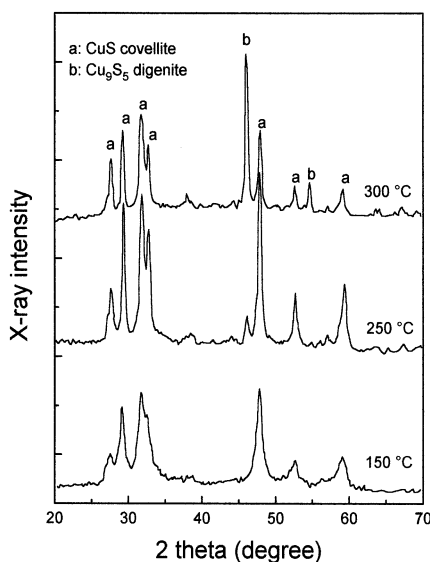


Fig. 20. Partial conversion of the CuS (covellite) precipitate in the composite coatings to Cu₉S₅ (digenite) when the coatings are annealed at 300°C.

the temperature dropping to nearly 150°C at the far end. The geometry of the vapor phase deposition set up is discussed in Ref. [69].

Fig. 21 shows that the film deposited at a substrate temperature of 345°C during 5 h from the bismuth sulfide precipitate maintained at 500°C presents well-defined peaks. Even though there is a general agreement of the peak positions with that of standard Bi₂S₃ (bismuthinite, JCPDS 17320), the intensity ratios observed in the film vary from that of the powder sample. This indicates preferential orientation of the crystallites. Fig. 22 shows the plot of the square of the product of the optical density (o.d) = (αd)/2.303 (where α is the absorption coefficient and d the thickness of the film) and the photon energy $E = hc/\lambda$ (where h is the Planck's constant; c the velocity of light; and λ the wavelength of radiation). The thin films possess a wide range of direct optical band gaps from 1.0 to 2.0 eV, depending on the temperature of the substrate. The range of photosensitivity, $S = (I_{ph} - I_d)/I_d = (\sigma_{ph} - \sigma_d)/\sigma_d$ (where I_{ph} and σ_{ph} are the photocurrent and photoconductivity, respectively, and I_d and σ_d are the dark current and dark conductivity, respectively) varies widely as shown in Fig. 23. High electrical conductivity is typical of films deposited at higher substrate temperatures. Thus, the optical and electrical properties of the films may be varied depending on the chosen substrate temperature to suit specific applications of the films.

3.9. Chemically deposited semiconductor thin films for solar energy related applications

Major advantages of the chemical bath deposition for solar energy applications: Two major characteristics of solar energy are well recognized: (i) It is abundant in most part

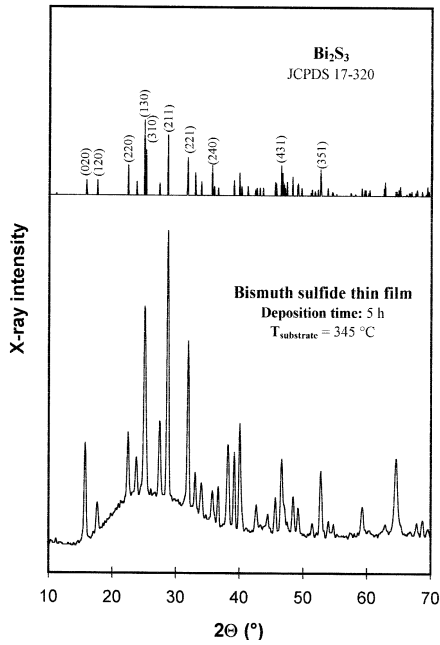
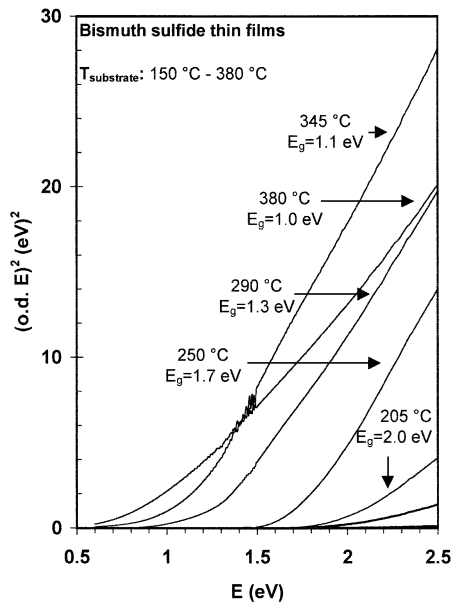


Fig. 21. XRD patterns of bismuth sulfide thin films deposited with substrate temperature of 345°C using bismuth sulfide precipitate as source, source temperature, 500°C at 4000 Pa. Standard patterns for Bi_2S_3 (bismuthinite) is given for the sake of comparison.



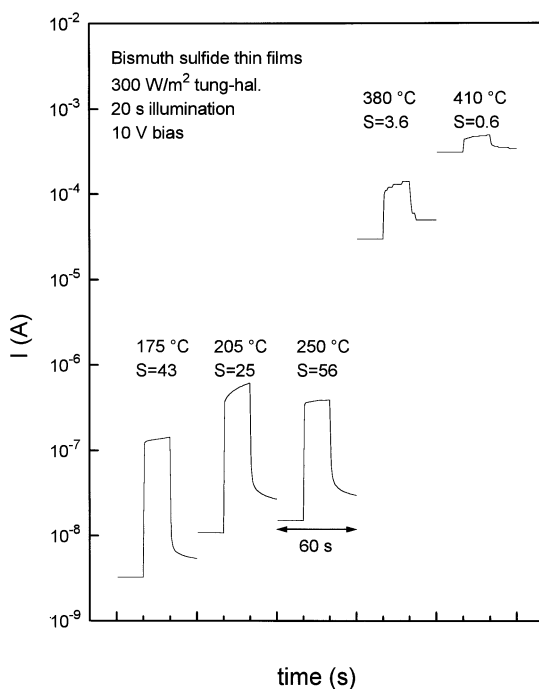


Fig. 23. Photocurrent response of bismuth sulfide thin films deposited from vapor phase at different substrate temperatures using bismuth sulfide precipitate as the source. The values of photosensitivity S are given.

of the world; and (ii) it is available in a relatively dilute form, typically $20 \text{ MJm}^{-2}/\text{day}$, as compared with nearly 30 MJ/kg obtainable from coal or petroleum. Collection of solar energy over a large area is inevitable. Chemical bath deposition is considered to be excellent in producing semiconductor thin films over large areas for such applications.

(i) *Application in solar control coatings*: In previous papers we have described the application of various chemically deposited semiconductor thin films for this purpose [12,13]. The basic purpose of this application is to reduce space cooling expenses in buildings and in automobiles by selectively controlling the amount of visible and infrared radiation entering through glazings. Chemically deposited CuS thin films have been found to possess near-ideal solar control characteristics: transmittance in the visible region of 20–50%, low transmittance, 10–20%, in the infrared region, low reflectance, $< 10\%$, in the visible region so as to avoid glare, and relatively higher reflectance, $> 15\%$, in the near-infrared region [70]. The coatings can be made on

Fig. 22. Variation in the optical band gap of bismuth sulfide thin films deposited at different substrate temperatures (205–380 °C) from vapor phase using bismuth sulfide precipitate as the source (source temperature, 500 °C; pressure: 4000 Pa).

sheet glass, acrylic, or polyester sheet and foils with equal ease [71]. To impart versatility and improvement of adhesion of the film to glass substrate, substrate films of chemically deposited PbS [72], SnS [73], ZnS [35], Bi₂S₃ [74], and ZnS–NiS [75] have been proposed. A major problem in the application of these films was the need for a protective coating. The use of an aromatic polyurethane-based commercial transparent varnish was tried with limited success [76].

We have recently concluded that the best way to use chemically deposited solar control coatings is in the form of a laminated glazing. In this configuration, coatings were made on 3 mm thick commercial sheet glass and then laminated using a commercially available laminating polymer sheet of 0.4 mm thickness. This is a proprietary copolymer [77] of polyvinyl butyryl-acetate – alcohol with other ingredients added in order to prevent degradation of the polymer by the ultraviolet component of solar radiation. The lamination, of glass + coating–polymer–clear sheet glass, was done in an autoclave at 140°C under 2 kg cm^{–2} pressure for about 3 h.

Fig. 24 illustrates the transmittance and reflectance spectra of two different coatings CuS and PbS–CuS, where the individual coating thicknesses are of the order of 0.1 μm. The spectra were recorded for incidence from the side of the coated glass – the recommended mode of incidence to minimize entry of the ultraviolet component of solar radiation into the polymer. The calculation of integrated reflectance (R) and transmittance (T) in the visible (vis) and infrared (ir) were calculated for air mass two solar spectrum as described in Ref. [12]. The implication of these values in the solar control parameters of the glazing is discussed in Ref. [13]. The visible transmittance, T_{vis} , of 51% and visible reflectance, R_{vis} , of 12% of the laminated CuS coatings are suitable for use in automobile glazing and combination of $T_{\text{vis}} = 21\%$, $R_{\text{vis}} = 18\%$, and $R_{\text{ir}} = 28\%$ of the laminated PbS–CuS coating are suitable for architectural glazing applications.

(ii) *Application as solar absorber coatings*: Chemically deposited SnS–CuS [78], PbS–CuS and Bi₂S₃–CuS [79] coatings have been investigated by us for application as absorber coating in all-glass tubular solar collectors. The efficiency of such coatings has been analyzed in a theoretical model [11]. It was apparent that the absorber coating must be located on the outside of the inner glass tube. The stability of the coating in the vacuum zone at operating temperature of 300°C is therefore the major issue to be addressed. In the case of PbS–CuS and ZnS–CuS thin films, thermal stability at temperatures of up to 350°C has been observed to be satisfactory during air annealing [5]. The solar absorptance of a PbS–CuS film is about 0.87 and thermal emittance is less than 0.46 (corresponding to sheet resistance of the annealed film of about 32 Ω□ [79]). As per theoretical prediction [11], such a coating can offer conversion efficiency of about 50% at an f -value of 0.1°C m² W^{–1}. This value is not very attractive compared to what may be offered by coatings produced by vacuum techniques [80]. However, the advantage of chemical bath deposition in producing uniform coatings on glass tubes is substantial over vacuum techniques. Further work on the thermal stability of chemically deposited multilayer films in vacuum at 300–400°C is worth considering to develop this application.

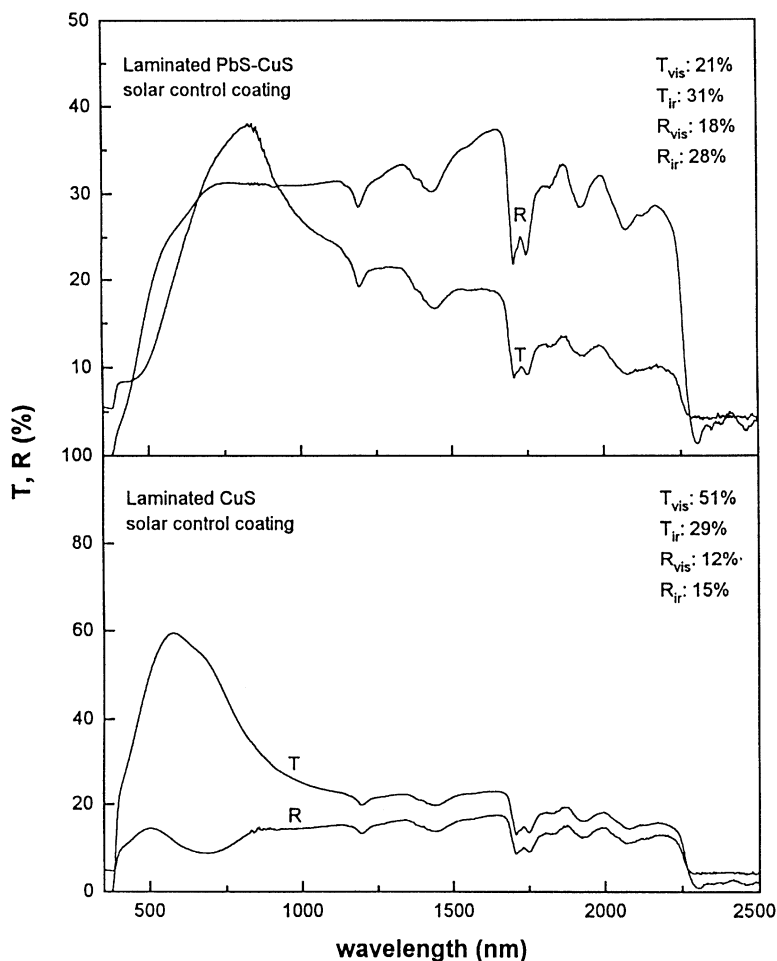


Fig. 24. Optical transmittance and reflectance of CuS and PbS–CuS coatings deposited on 3 nm thick commercial window glass and laminated with a clear window glass (3 mm) using commercial-grade laminating polymer [77]. Laminating process: 140°C under 2 kg/cm² pressure for 2 h.

(iii) *Photodetector and photovoltaic applications:* Fig. 25 shows the dependence of the photoresponse curve of chemically deposited CdSe thin films as a function of the intensity of illumination. The dependence of the photocurrent on the intensity is nearly linear. The photo generation of such magnitude in the depletion layer of a Schottky barrier or p–n, p–i–n junction leads to the build up of photo voltage. We consider that the possibility of creating new materials through interfacial diffusion of atoms in chemically deposited multilayer stacks as demonstrated in PbS–CuS, ZnS–CuS and Bi₂S₃–CuS films [5,6] is very high. Table 1 suggests a list of possible absorber materials for photovoltaic application chosen from the data given in

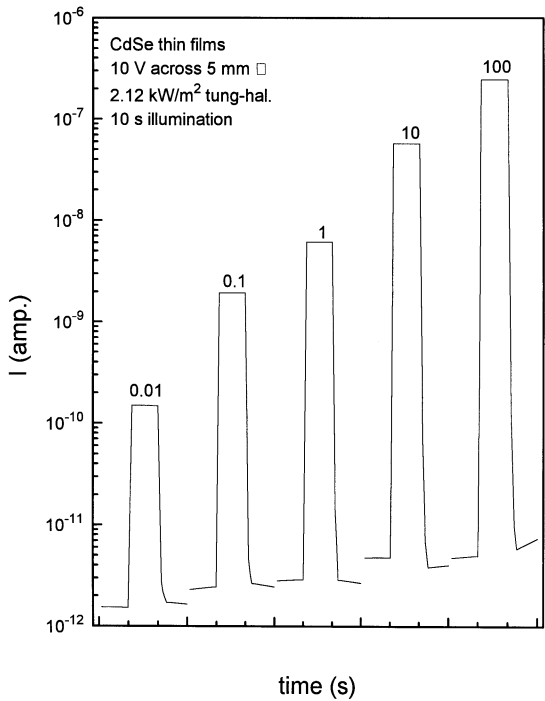


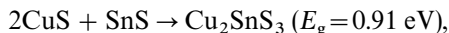
Fig. 25. Photoresponse curves of a CdSe thin film annealed in air at 450°C at different illumination levels (0.01%), 0.2 W m⁻² and to 100%, 2.12 kW m⁻² illustrating near-linear dependence of photocarrier generation on the intensity of illumination – a basic feature on which photovoltaic effect depends.

Table 1

Suggestions for the development of new solar cell/solar energy materials which may be prepared through the interfacial diffusion of ions in multilayer chemically deposited thin films during annealing. The data have been extracted from Ref. [43]

Material	Structure	Band gap (eV)	Hole mobility (cm ² /Vs)
CuSbSe ₂	Orthorhombic	0.83	5
AgSbS ₂	Monocl.	1.73	1500
AgSbSe ₂	Rock salt	0.58	
AgBiS ₂	Rock salt	0.9	
Cu ₃ SbS ₄	Zincblende	0.46	
Cu ₃ SbSe ₄	Zincblende	0.31	50
Ag ₂ SnSe ₃		0.81	910
Cu ₂ SnSe ₃		0.96	870
Cu ₂ SnS ₃		0.91	605
PbSnS ₃		1.05	

Ref. [43], which may be produced by solid-state reaction of the type



etc., where the CuS [42], SnS [37], PbS [38], Bi₂S₃ [39] Ag₂S [81] Sb₂S₃ [48] films are produced by chemical bath deposition. In the case of SnS and SnS₂, it has been reported that by controlling the bath composition and temperature either of the composition may be obtained [82]. Further, new materials may also be created by combining chemical deposition technique with thermal evaporation or sputtering of metals, for example, Sb₂S₃ + 3CuS + 3Cu → 2Cu₃SbS₃, etc. We consider that creation of new thin-film materials by the above approaches is vital for the further advancement of the chemical bath deposition technique and integration of the films produced in this way into solar energy technologies.

3.10. Toxicity considerations

The chemical deposition technique involves the use of dilute solutions of compounds involved in the reaction. This offers minimum toxicity and occupational hazards since the vapor phase of the reactants are avoided. It is well known that toxicity hazards associated with lead, cadmium, mercury, selenium, etc, are severe when inhaled [83]. An analysis on the toxicity hazard in the production of chemically deposited PbS thin films is given in Ref. [84] where it was established that the chemical bath technique does not entail the usual health hazards associated with lead pollution. Further, the unreacted ions can be precipitated in the bath as sulfides or selenides and the solid can be separated and stored for use as discussed above in Section 3.8 or recycled to produce starting material. The formation of multinary compounds by interfacial diffusion and recrystallization in multilayer films as given above can be considered as an environmentally sound process since very few effluents are produced. Overall, the large area capability and the ease of scaling up with complete control of material handling in solid or liquid phase offers perspective toward the industrial production of coatings and devices by the chemical bath deposition technique.

4. Conclusions

In this paper we presented a perspective on the chemically deposited thin films: the deposition technique, post-deposition processing, the use of precipitate and an overview of the applications related to solar energy utilization. We consider that this research area offers immense possibilities in creating new materials by annealing multilayer film or combining chemically deposited films with vacuum-deposited metallic films. Future research efforts may be directed in this direction.

Acknowledgements

The authors are grateful to Leticia Baños of the Instituto de Investigaciones en Materiales, UNAM, for recording the XRD patterns. Financial support for this work was received from CONACYT, México through 1816-E9211 and from DGAPA-UNAM through IN-502594 and IN-501495. One of us (V.M.G) is grateful to the Universidad Autonoma de Zacatecas for financial support.

References

- [1] O. Houser, E. Beisalski, *Chem-Ztg.* 34 (1910) 1079.
- [2] K.L. Chopra, R.C. Kainthla, D.K. Pandya, A.P. Thakoor, in: G. Hass, M.H. Francombe, J.L. Vossen (Eds.), *Physics of Thin Films*, vol. 12, Academic Press, New York, 1982, p. 201.
- [3] C.D. Lokhande, *Mater. Chem. Phys.* 27 (1991) 1–43.
- [4] I. Grozdanov, *Semicond. Sci. Technol.* 9 (1994) 1234.
- [5] L. Huang, P.K. Nair, M.T.S. Nair, R.A. Zingaro, E.A. Meyers, *J. Electrochem. Soc.* 141 (1994) 2536.
- [6] P.K. Nair, L. Huang, M.T.S. Nair, Hailin Hu, E.A. Meyers, R.A. Zingaro, *J. Mater. Res.* 12, 1997, (in Press).
- [7] D.E. Bode, in: G. Hass, R.E. Thun (Eds.), *Physics of Thin Films*, vol. 3, Academic Press, New York, 1966, p. 275.
- [8] A.G. Stanley, *Cadmium Sulfide Solar Cells*, in: R. Wolf (Ed.), *Applied Solid State Sciences*, vol. 5, Academic Press, New York, 1975, p. 251.
- [9] S.V. Svechnikov, E.B. Kaganovich, *Thin Solid Films* 66 (1980) 41.
- [10] G.B. Reddy, V. Dutta, D.K. Pandya, K. L. Chopra, *Sol. Energy Mater.* 15 (1987) 383; 15 (1987) 153.
- [11] C. Estrada-Gasca, G. Alvarez-García, R.E. Cabanillas, P.K. Nair, *Renewable Energy* 2 (1992) 477; *J. Phys. D* 25 (1992) 1142.
- [12] P.K. Nair, M.T.S. Nair, A. Fernández, M. Ocampo, *J. Phys. D* 22 (1989) 829.
- [13] C. Estrada-Gasca, G. Alvarez-García, P.K. Nair, *J. Phys. D* 26 (1993) 1304.
- [14] R.A. Boudreau, R.D. Rauh, *J. Electrochem. Soc.* 130 (1983) 513.
- [15] M.E. Rincón, M. Sánchez, A. Olea, I. Ayala, P.K. Nair, Photoelectrochemical behavior of thin CdS, coupled CdS/CdSe semiconductor thin films, *Solar Energy Mater. Solar Cells* (1997), These proceedings.
- [16] O. Savadogo, Chemically and electrochemically deposited thin films for solar energy materials, *Solar Energy Mater. Solar Cells* (1997) These proceedings.
- [17] Bluent Basol, Vijay Kapur, *IEEE Trans. Electron Dev.* 37 (1990) 418.
- [18] T.R. Tuttle, M.A. Contreras, J.S. Ward, A.L. Tennant, K.R. Ramanathan, J. Keane, R. Noufi, in: C.M. Lampert et al. (Ed.), *Proc. SPIE*, vol. 2531, SPIE, Bellingham, 1995, p. 194.
- [19] M.A. Mickelsen, W.S. Chen, *Appl. Phys. Lett.* 36 (1980) 371.
- [20] A. Rothwarf, *Proc. 16th IEEE Photovoltaic Specialists Conf.*, San Diego, CA, IEEE, New York, 1982, p. 791.
- [21] B.M. Basol, V.K. Kapur, A. Halani, C. Leidholm, in: K.A. Summers (Ed.), *Annual Report, Photovoltaic Subcontract Program FY 1991*, Golden, NREL, p. 50.
- [22] O. Savadogo, K.C. Mandal, *Appl. Phys. Lett.* 63 (1993) 12.
- [23] O. Savadogo, K.C. Mandal, *J. Electrochem. Soc.* 141 (1994) 2871.
- [24] O. Savodogo, K.C. Mandal, *J. Phys. D* 27 (1994) 1070.
- [25] P.K. Nair, V.M. García, A.B. Hernandez, M.T.S. Nair, *J. Phys. D* 24 (1991) 1466.
- [26] P.K. Nair, O. Gomezdaza, M.T.S. Nair, *Adv. Mater. Opt. Electron.* 1 (1992) 139.
- [27] P.K. Nair, M.T.S. Nair, O. Gomezdaza, R.A. Zingaro, *J. Electrochem. Soc.* 140 (1993) 1085.
- [28] J. Basset, R.C. Denney, G.H. Jeffery, J. Mendham, in: *Vogel's Textbook of Quantitative Inorganic Analysis*, 4th ed., ELBS/Longman, London, 1978, p. 25.

- [29] D.R. Lide, (Editor-in-Chief), CRC Handbook of Chemistry and Physics 76th Ed., CRC Press, Boca Raton, 1995-96, pp. 8-58.
- [30] J. Bjerrum, B.V. Agarwala, S. Refn., *Acta Chem. Scand. A* 35 (1981) 685.
- [31] N.R. Pavaskar, C.A. Menezes, A.B.P. Sinha, *J. Electrochem. Soc.* 124 (1977) 743.
- [32] M.T.S. Nair, P.K. Nair, R.A. Zingaro, E.A. Meyers, *J. Appl. Phys.* 75 (1994) 1557.
- [33] M.T.S. Nair, P.K. Nair, H.M.K.K. Pathirana, R.A. Zingaro, E.A. Meyers, *J. Electrochem. Soc.* 140 (1993) 2987.
- [34] V.M. García, M.T.S. Nair, P.K. Nair, R.A. Zingaro, *Semicond. Sci. Technol.* 11 (1996) 427.
- [35] P.K. Nair, M.T.S. Nair, *Semicond. Sci. Technol.* 7 (1992) 239.
- [36] C.A. Estrada, P.K. Nair, M.T.S. Nair, R.A. Zingaro, E.A. Meyers, *J. Electrochem. Soc.* 141 (1994) 802.
- [37] M.T.S. Nair, P.K. Nair, *Semicond. Sci. Technol.* 6 (1991) 132.
- [38] P.K. Nair, M. Ocampo, A. Fernandez, M.T.S. Nair, *Sol. Energy Mater.* 20 (1990) 235; V.M. García, M.T.S. Nair, P.K. Nair, *Sol. Energy Mater.* 23 (1991) 47.
- [39] M.T.S. Nair, P.K. Nair, *Semicond. Sci. Technol.* 5 (1990) 1225.
- [40] P.K. Nair, J. Campos, A. Sánchez, L. Baños, M.T.S. Nair, *Semicond. Sci. Technol.* 6 (1991) 393.
- [41] V.M. García, M.T.S. Nair, P.K. Nair, R.A. Zingaro, *Semicond. Sci. Technol.* 12 (1997) (May issue), in press.
- [42] P.K. Nair, V.M. García, A.M. Fernández, H.S. Ruiz, M.T.S. Nair, *J. Phys. D* 24 (1991) 441.
- [43] O. Madelung, in: *Semiconductors other than Group IV elements, III–V compounds*, Springer, Berlin, 1992.
- [44] M. Moskovits, in: G. Soles (Ed.), *Chemical Physics of Atomic and Molecular Clusters*, North Holland, Amsterdam, 1990, p. 397.
- [45] For example, M.N. Rudden, J. Wilson, *Elements of Solid State Physics*, Wiley, Chichester, 1980, p. 59.
- [46] L. Brus, *J. Chem. Phys.* 90 (1986) 2555.
- [47] G. Hodes, A.A. Yaron, F. Decker, P. Motisuke, *Phys. Rev. B* 36 (1987) 4215.
- [48] K.C. Mandal, O. Savadogo, *Sol. Energy Mater. Sol. Cells* 26 (1992) 117.
- [49] K. Okamoto, S. Kawai, *Jpn. J. Appl. Phys.* 12 (1973) 1130; J.J. Loferski, J. Schewchun, S.D. Mittleman, E.A. DeMeo, R. Arnott, H.L. Hwang, R. Beaulieu, G. Chapman, *Sol. Energy Mater.* 1 (1979) 157.
- [50] H.S. Randhawa, R.F. Bunshah, D.G. Brock, B.M. Basol, O.M. Staffsudd, *Sol. Energy Mater.* 6 (1982) 445.
- [51] M.T.S. Nair, P.K. Nair, *Semicond. Sci. Technol.* 4 (1989) 191.
- [52] J.W. Orton, B.J. Goldsmith, J.A. Chapman, M.J. Powell, *J. Appl. Phys.* 53 (1982) 1602.
- [53] M.V. García-Cuenca, J.L. Morenza, J.M. Cordina, *J. Phys. D* 20 (1987) 951.
- [54] R.L. Call, N.K. Jaber, K. Seshan, J.R. Whyte, *Sol. Energy Mater.* 2 (1980) 373.
- [55] P.K. Nair, M.T.S. Nair, R.A. Zingaro, E.A. Meyers, *Thin Solid Films* 239 (1994) 85.
- [56] M.T.S. Nair, P.K. Nair, H.M.K.K. Pathirana, R.A. Zingaro, E.A. Meyers, *J. Electrochem. Soc.* 140 (1993) 2987.
- [57] P.J. George, A. Sánchez, P.K. Nair, M.T.S. Nair, *Appl. Phys. Lett.* 66 (1995) 3624.
- [58] P.J. George, A. Sánchez-Juarez, P.K. Nair, *Semicond. Sci. Technol.* 11 (1996) 1090.
- [59] V.M. García, P.J. George, M.T.S. Nair, P.K. Nair, *J. Electrochem. Soc.* 143 (1996) 2892.
- [60] M. Savelli, J. Bougnot, in: B.O. Seraphin (Ed.), *Solar Energy Conversion and Topics in Applied Physics*, vol. 31, Springer, Berlin, 1979, p. 213.
- [61] C.A. Estrada, R.A. Zingaro, E.A. Meyers, P.K. Nair, M.T.S. Nair, *Thin Solid Films* 247 (1994) 208.
- [62] P.K. Nair, M.T.S. Nair, H.M.K.K. Pathirana, R.A. Zingaro, E.A. Meyers, *J. Electrochem. Soc.* 140 (1993) 754.
- [63] K.L. Chopra, S.R. Das, in: *Thin Film Solar Cells*, Plenum, New York, 1982, p. 233.
- [64] H. Matsumoto, K. Kuribayashi, H. Uda, Y. Komatsu, A. Nakamoto, S. Ikegami, *Sol. Cells* 11 (1984) 367.
- [65] O. Gomezdaza, V.M. García, M.T.S. Nair, P.K. Nair, *Appl. Phys. Lett.* 68 (1996) 1987–1989.
- [66] P.K. Nair, M.T.S. Nair, J. Campos, L.E. Sansores, *Sol. Cells* 22 (1987) 213.
- [67] M.T.S. Nair, P.K. Nair, J. Campos, *Thin Solid Films* 161 (1988) 21.
- [68] H. Hu, J. Campos, P.K. Nair, *J. Mater. Res.* 11 (1996) 739.
- [69] M.E. Rincon, P.K. Nair, *Semicond. Sci. Technol.* 12 (1997) at Press.

- [70] M.T.S. Nair, P.K. Nair, *Semicond. Sci. Technol.* 4 (1989) 599.
- [71] H. Hu, P.K. Nair, *Surface Coating Technol.* 81 (1996) 183.
- [72] P.K. Nair, M.T.S. Nair, *Semicond. Sci. Technol.* 4 (1989) 807.
- [73] M.T.S. Nair, P.K. Nair, *J. Phys. D* 24 (1991) 450.
- [74] M.T.S. Nair, G. Alvarez-Garcia, C. Estrada-Gasca, P.K. Nair, *J. Electrochem. Soc.* 140 (1993) 212.
- [75] A.M. Fernandez, M.T.S. Nair, P.K. Nair, *Mater. Manufr. Process* 8 (1993) 535.
- [76] A.M. Fernandez, P.K. Nair, *Thin Solid Films* 204 (1991) 459.
- [77] Vitro Vidrio Plano-Industria Quimica M, S.A. de C.V., Tlaxcala-Puebla, Tlaxcala C.P.90780 AP 942 México.
- [78] P.K. Nair, M.T.S. Nair, *J. Phys. D* 24 (1991) 83.
- [79] V.M. Garcia, M.T.S. Nair, P.K. Nair, *Solar Energy Mater.* 23 (1991) 47.
- [80] B. Window, *Solar Energy* 31 (1983) 159.
- [81] A.J. Varkey, *Solar Energy Mater.* 21 (1991) 291.
- [82] R.D. Engelken, H.E. McCloud, C. Lee, M. Slayton, A. Ghreishi, *J. Electrochem. Soc.* 134 (1987) 2696.
- [83] N.I. Sax, *Dangerous properties of Industrial Materials*, 6th ed., Van Nostrand, Reinhold, New York, 1984, p. 612, 1693, 1751, 2390.
- [84] P.K. Nair, M.T.S. Nair, *J. Phys. D* 23 (1990) 150.